Available online at www.sciencedirect.com
ScienceDirect
Journal of Power Sources 177 (2008) 254–261
JOURNAL OF POWER SOURCES
www.elsevier.com/locate/jpowsour

Electrochemical study of a planar solid oxide fuel cell: Role of support structures

Yaneeporn Patcharavorachot, Amornchai Arpornwichanop*, Anon Chuachuensuk

Department of Chemical Engineering, Faculty of Engineering, Chulalongkorn University, Bangkok 10330, Thailand

Received 13 July 2007; received in revised form 10 October 2007; accepted 22 November 2007
Available online 4 December 2007

Abstract

This paper presents a performance analysis of a planar solid oxide fuel cell (SOFC) with different support structures, i.e., electrode (anode and cathode) and electrolyte supports. An electrochemical model, taking into account structural and operational parameters and gas diffusion at the electrodes, is used to analyze the characteristics of the planar SOFC. Simulation results demonstrate that under cell operation at an intermediate temperature (1073 K), an anode-supported SOFC is superior to an electrolyte- and cathode-supported SOFC. Analysis of individual cell voltage loss indicates that ohmic loss dominates the performance of an electrolyte-supported SOFC whereas activation and ohmic overpotentials constitute the major loss in an electrode-supported counterpart. Sensitivity analyses of the anode-supported SOFC show that decreasing the electrolyte and anode thickness can improve cell performance. A decrease in operating temperature causes the cell to operate at a lower range of current density due to an increase in ohmic and activation overpotentials. Further, increasing the operating pressure and degree of pre-reforming reduces the concentration overpotential and thereby enhances cell performance.

Keywords: Planar solid oxide fuel cell; Support structure; Electrochemical model; Performance analysis; Overpotential

1. Introduction

A fuel cell is an energy-conversion device that produces electricity and heat directly from chemical conversion of a fuel gas and an oxidant via an electrochemical reaction. Among the various types of fuel cell, the solid oxide fuel cell (SOFC) has attracted considerable interest for distributed power sources due to its high efficiency and low emission of pollutants to the environment [1,2]. The high-temperature operation of SOFCs offers many advantages that include a high electrochemical reaction rate, the flexibility of using various fuel types (i.e., methane, methanol, ethanol, etc.), a tolerance to impurities, the prospect for combined heat and power systems [3,4].

In general, a SOFC can have either a planar or tubular configuration. The planar design has recently received much attention since it is simpler to fabricate and more flexible in terms of cell geometry (i.e., circular or prismatic) and gas manifolding (i.e., co-, counter- and cross-flow direction) [5]. In addition, due to the fact that its short current path results in low-internal electrical resistances, a planar SOFC provides higher power density, compared with a tubular design [6]. Currently, two basic approaches are proposed in the development of the planar SOFC. In an electrolyte-supported SOFC, the electrolyte is the thickest component (>150 μm) while the anode and cathode are very thin (about 50 μm) [7,8], which results in high ohmic resistance. Thus, most current research efforts have been focused on the application of the electrolyte-supported SOFCs at a high operating temperature. In an electrode-supported SOFC, one of the two electrodes, either the cathode or the anode, is the thickest component (around 2 mm) and support structure [7]. This decreases the ohmic resistance and makes the design better suited for operation at lower temperatures (873–1073 K); the system is referred to as an 'intermediate-temperature solid oxide fuel cell' (IT-SOFC). The development and performance improvement of the IT-SOFC have received much attention due to several potential benefits, e.g., the possibility of using a wider range of materials and the promise of low-cost fabrication.

Considering the characteristics of the electrode-supported SOFC, it has been reported that activation and concentration

* Corresponding author. Tel.: +66 2 2186878; fax: +66 2 2186877.
E-mail address: Amornchai.A@chula.ac.th (A. Arpornwichanop).

0378-7753/$ – see front matter © 2007 Elsevier B.V. All rights reserved.
doi:10.1016/j.jpowsour.2007.11.079

Nomenclature

D_{eff}	electrode effective diffusion coefficient ($m^2\ s^{-1}$)
E	operating voltage (V)
$E_{\text{electrode}}$	activation energy of the exchange current density ($kJ\ mol^{-1}$)
E^{OCV}	open-circuit voltage (OCV) (V)
E^0	OCV at standard temperature and pressure and pure reactants for the H_2 oxidation reaction (V)
F	Faraday's constant ($C\ mol^{-1}$)
i	current density ($A\ m^{-2}$)
$i_{0,\text{electrode}}$	exchange current density ($A\ m^{-2}$)
n	number of electrons participating in the electrochemical reaction
p_{i}	partial pressure of gas (kPa)
P	pressure (kPa)
R_{ohm}	internal resistance ($\Omega\ m^2$)
$\Re$	gas constant ($kJ\ mol^{-1}\ K^{-1}$)
T	temperature (K)

Greek symbols

α	transfer coefficient
η_{act}	activation overpotential (V)
η_{con}	concentration overpotential (V)
η_{ohm}	ohmic overpotential (V)
σ	electronic conductivity of electrode or ionic conductivity of electrolyte ($\Omega^{-1}\ m^{-1}$)
τ_{anode}	anode thickness (m)
τ_{cathode}	cathode thickness (m)
$\tau_{\text{electrolyte}}$	electrolyte thickness (m)

overpotentials can often outweigh the benefit of reduced ohmic loss due to smaller electrolyte thickness so that the specific resistance of the electrode-supported SOFC at an intermediate temperature may be larger than that of the high-temperature SOFC. Further, it is well known that the performance characteristics of SOFCs are strongly affected not only by operating conditions such as temperature and pressure, and fuel and oxidant composition but also by structural parameters such as the thickness of electrodes and electrolyte and the porosity of electrodes. Therefore, the performance analysis of fuel cells should take these parameters into account as it will lead to an optimum design and operation of SOFCs.

In this study, the role of the support structure and the influence of operating parameters on the performance of a planar SOFC are investigated by considering its electrical characteristics obtained from a detailed electrochemical model. Most previous studies on the performance analysis of a fuel cell have been carried out based on a simple model to characterize the SOFC overpotentials [9,10]. Here, the non-linear Butler–Volmer equation is employed to describe the activation overpotential instead of using the simplified Tafel equation and the exchange-current density is dependent on the operating temperature. The ohmic overpotential is related to cell structural parameters, i.e., the thickness of cell components, and ionic and electronic conductivities that are changed by the operating temperature. Gas diffusion through the porous electrodes is considered in the determination of the concentration overpotential.

2. Electrochemical model

A single planar SOFC consists of a dense ceramic electrolyte sandwiched between two porous electrodes (anode and cathode) as illustrated in Fig. 1. The most common materials used for the SOFC cell components are oxide ion conducting yttria-stabilized zirconia (YSZ) for the electrolyte, strontium-doped lanthanum manganite (LSM) for the cathode, and nickel/YSZ for the anode. During fuel cell operation, oxidant gas (oxygen or air) at the cathode side receives electrons to form oxygen ions that migrate through the electrolyte to the electrolyte|anode interface. Fuel gas (possibly pure H_2 or H_2-rich gas) simultaneously fed at the anode side reacts with the oxygen ions to generate steam and electrons. The electron flow in the external circuit from the anode to the cathode produces direct-current electricity.

2.1. Reversible fuel cell voltage

In general, the difference between the thermodynamic potentials of the electrode reactions determines the reversible cell voltage, which is also known as the 'electromotive force (emf)' or 'reversible open-circuit voltage (E^{OCV})'. E^{OCV} is a theoretical voltage that drives charges around the circuit. For the SOFC system, it can be expressed by the Nernst equation, i.e.,

$$E^{\text{OCV}} = E^0 - \frac{\Re T}{2F} \ln\left(\frac{p_{\text{H}_2\text{O}}}{p_{\text{H}_2} p_{\text{O}_2}^{0.5}}\right) \quad (1)$$

where E^0 is the open-circuit voltage at the standard pressure and is a function of the operating temperature that can be expressed by the following equation [11]:

$$E^0 = 1.253 - 2.4516 \times 10^{-4} T \quad (2)$$

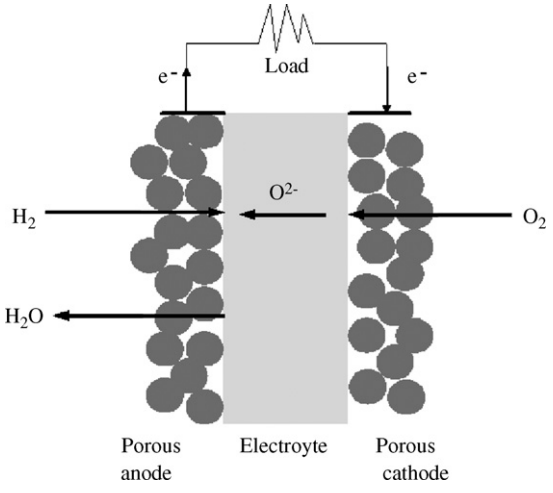

Fig. 1. Schematic diagram of solid oxide fuel cell.

2.2. Actual fuel cell voltage

When a current is drawn from a fuel cell, the operating cell voltage or actual fuel cell voltage, E, is less than the open-circuit voltage, as shown in Eq. (3). This is due to internal resistance and overpotential losses associated with the electrochemical reactions at the electrode|electrolyte interface. These various losses will be described as follows:

$$E = E^{\mathrm{OCV}} - (\eta_{\mathrm{act}} + \eta_{\mathrm{ohm}} + \eta_{\mathrm{conc}}) \tag{3}$$

Ohmic loss (η_{ohm}) occurs because of the electrical resistance of the electrodes and the resistance to the flow of ions in the electrolyte. This loss is important in all types of fuel cell and is proportional to the current density (i) as given by:

$$\eta_{\mathrm{ohm}} = iR_{\mathrm{ohm}} \tag{4}$$

where R_{ohm} is the internal resistance of the cell that can be estimated from the effective distance between the cell components coupled with conductivity data, as given by [12]:

$$R_{\mathrm{ohm}} = \frac{\tau_{\mathrm{anode}}}{\sigma_{\mathrm{anode}}} + \frac{\tau_{\mathrm{electrolyte}}}{\sigma_{\mathrm{electrolyte}}} + \frac{\tau_{\mathrm{cathode}}}{\sigma_{\mathrm{cathode}}} \tag{5}$$

where τ and σ are the thickness and the conductivity of each cell component, respectively.

Activation overpotential (η_{act}) is the loss caused by electrochemical reactions at the electrode surfaces. Although the activation overpotential tends to be small at high temperatures owing to high reaction rates, it can become the most important cause of a cell voltage drop when the operating temperature is reduced. In this study, the non-linear Butler–Volmer equation (Eq. (6)) is used to describe the activation overpotential, namely:

$$i = i_{0,\mathrm{electrode}} \left[\exp\left(\frac{\alpha n F}{\Re T} \eta_{\mathrm{act,electrode}} \right) - \exp\left(-\frac{(1-\alpha) n F}{\Re T} \eta_{\mathrm{act,electrode}} \right) \right] \tag{6}$$

where α is the transfer coefficient (=0.5), n the number of electrons transferred in the rate-limiting reaction step, and $i_{0,\mathrm{electrode}}$ is the electrode exchange-current density which depends on the operating temperature as shown in Eq. (7). Table 1 gives the values of the pre-exponential factor and the activation energy used for computing $i_{0,\mathrm{electrode}}$ [12]:

$$i_{0,\mathrm{electrode}} = \frac{\Re T}{nF} k_{\mathrm{electrode}} \exp\left(-\frac{E_{\mathrm{electrode}}}{\Re T} \right)$$
$$\mathrm{electrode} \in \{\mathrm{anode}, \mathrm{cathode}\} \tag{7}$$

Table 1
Values of pre-exponential factor and activation energy for computing exchange-current density

k_{cathode}	$2.35 \times 10^{11}\ \Omega^{-1}\ \mathrm{m}^{-2}$
k_{anode}	$6.54 \times 10^{11}\ \Omega^{-1}\ \mathrm{m}^{-2}$
E_{cathode}	$137\ \mathrm{kJ\ mol}^{-1}$
E_{anode}	$140\ \mathrm{kJ\ mol}^{-1}$

During operation of a fuel cell, concentration gradients develop across the electrodes, resulting in a lower concentration of reactants at the electrode|electrolyte interface and concentration overpotential (η_{conc}). This loss is more pronounced when fuel or oxidant gases with low purities are fed to a fuel-cell stack. The concentration overpotential can be evaluated by the following expression:

$$\eta_{\mathrm{conc}} = \frac{\Re T}{2F} \ln\left(\frac{p_{\mathrm{H_2O,TPB}}}{p_{\mathrm{H_2O}}} \frac{p_{\mathrm{H_2}}}{p_{\mathrm{H_2,TPB}}} \right) + \frac{\Re T}{4F} \ln\left(\frac{p_{\mathrm{O_2}}}{p_{\mathrm{O_2,TPB}}} \right) \tag{8}$$

where the first term on the right-hand side refers to the anode concentration overpotential ($\eta_{\mathrm{conc,anode}}$) and the second term refers to the cathode concentration overpotential ($\eta_{\mathrm{conc,cathode}}$). The partial pressures of H_2, H_2O, and O_2 at the interface calculated using a gas transport model in porous media can be expressed as [12]:

$$p_{\mathrm{H_2,TPB}} = p_{\mathrm{H_2}} - \frac{\Re T \tau_{\mathrm{anode}}}{2F \overline{D}_{\mathrm{eff,anode}}} i \tag{9}$$

$$p_{\mathrm{H_2O,TPB}} = p_{\mathrm{H_2O}} + \frac{\Re T \tau_{\mathrm{anode}}}{2F \overline{D}_{\mathrm{eff,anode}}} i \tag{10}$$

$$p_{\mathrm{O_2,TPB}} = P - (P - p_{\mathrm{O_2}}) \exp\left(\frac{\Re T \tau_{\mathrm{cathode}}}{4F \overline{D}_{\mathrm{eff,cathode}} P} i \right) \tag{11}$$

It is noted that in this study, the effect of the variation of the gas-diffusion coefficient with a temperature is not included in Eqs. (9)–(11) for computing the concentration overpotentials. Although the gas-diffusion coefficient increases with increasing temperature, the effect of increased diffusion rate on the concentration overpotential is less pronounced [11]. Therefore, the gas-diffusion coefficient is assumed to be constant.

3. Results and discussion

An analysis of the effects of design and operating parameters on the performance characteristics of a fuel cell provides important information for producing a cell with optimum investment and operating costs. In this section, the influence of support structures and key operating parameters on SOFC performance under isothermal conditions is presented. Table 2 shows the values of the cell geometry and material properties used in the study whereas the operating conditions are listed in Table 3 [12,13]. The fuel composition given in Table 3 is based on the gas mixture obtained from an external reformer fed by steam and methane at a ratio of 2. The methane steam reforming and water gas shift reactions are assumed to be at equilibrium. It is noted that an external reformer is usually installed before the SOFC system in order to produce hydrogen-rich feed and to reduce the possibility of carbon formation on the anode. The ionic conductivity of the electrolyte and the anode and cathode electronic conductivities are considered to be temperature dependent [13]. The effective diffusivity coefficients are calculated assuming electrodes with 30% porosity ($\varepsilon_{\mathrm{p}} = 0.30$), a tortuosity of $\tau_{\mathrm{tortuosity}} = 6$, and an average pore radius (used to calculate the Knudsen diffusivity) of 0.5 μm [12].

Table 2
Values of structural and material property parameters for planar SOFC

Parameters	Anode	Electrolyte	Cathode
A-S structure[a] (μm)	500	40	40
C-S structure[b] (μm)	40	40	500
E-S structure[c] (μm)	40	500	40
σ[d] (Ω^{-1} m^{-1})	$\frac{4.2\times10^7}{T}\exp\left(-\frac{1200}{T}\right)$	$33.4\times10^3\exp\left(-\frac{10300}{T}\right)$	$\frac{9.5\times10^7}{T}\exp\left(-\frac{1150}{T}\right)$
D_{eff} (m^2 s^{-1})	3.66×10^{-5}	–	1.37×10^{-5}

[a] A-S structure: anode-supported SOFC.
[b] C-S structure: cathode-supported SOFC.
[c] E-S structure: electrolyte-supported SOFC.
[d] Ionic conductivity for electrolyte and electronic conductivity for electrode.

Table 3
Operating conditions for SOFC under standard condition

Parameter	Value
Operating temperature, T (K)	1073
Operating pressure, P (atm)	1
Fuel composition[a]	30% H_2, 42.3% H_2O, 19.7% CH_4, 3% CO and 5% CO_2
Air composition	21% O_2 and 79% N_2

[a] Fuel composition is based on a fully reformed steam and methane mixture with a steam:carbon ratio = 2.

3.1. Role of support structures

The performance characteristics of an anode-supported SOFC under isothermal operation (T = 1073 K) at different operating current densities (i) are presented in Fig. 2. The cell voltage decreases with increase in operating current density due to the increased voltage losses from the irreversible SOFC cell resistance. The power density increases initially to a maximum value of 0.69 W cm^{-2} at a current density of 1.5 A cm^{-2} and then slightly decreases to zero at 3.17 A cm^{-2}. This indicates that the cell performance is not controlled by the concentration loss under these operating conditions. It should be noted that in this study, the fuel and oxidant are assumed to be undepleted. Since, however, the fuel and air compositions vary along the length of the cell under real operation, due to fuel and oxygen utilization by electrochemical reactions, the actual cell performance is lower than the predicted value.

The ohmic and cathode activation overpotentials represent a major loss in cell voltage, followed by the anode activation overpotential (Fig. 2). The activation overpotential at the cathode side is generally higher than that at the anode side due to the lower exchange-current density. From this result, although the anode-supported SOFC is considered, the anode concentration overpotential is relatively small, compared with the other overpotenials. It is noted that the approximate expression (Eq. (7)) proposed by Aguiar et al. [12] was used to determine the value of the exchange-current density, which depends only on the operating temperature. In previous studies of the electrode

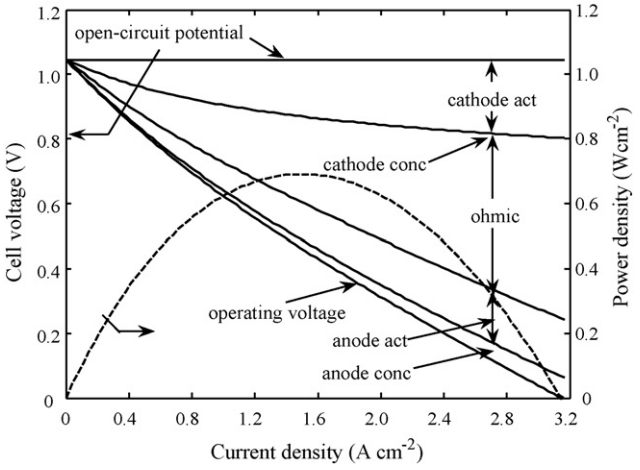

Fig. 2. Performance of anode-supported SOFC at different current densities.

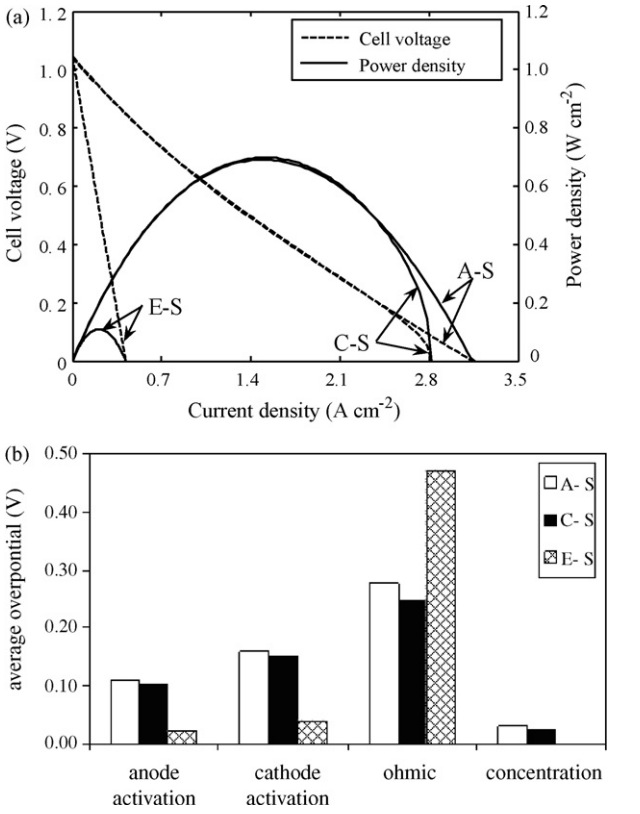

Fig. 3. Comparison of SOFC with different support structures: (a) cell performance and (b) individual overpotentials in cell.

reactions, however, it was reported that the exchange-current density depends on the partial pressures of hydrogen and oxygen [14,15,4] in addition to the operating temperature [16,17]. Therefore, if the effect of the gas partial pressure is taken into account, the calculated value of the exchange-current density will be reduced as it is directly proportional to the partial pressure of gas at the electrode|electrolyte interface. This results in a higher activation potential.

A comparison of SOFC performance with different support structures (i.e., anode-, cathode- and electrolyte-supported) is given in Fig. 3a. It is clearly shown that the performance of the electrode-supported SOFC is superior to that of the electrolyte-supported SOFC. The electrode-supported SOFC can operate at a higher power density and a wider range of current density, thus implying that a smaller cell area would be required to operate the SOFC system. In order to explain the influence of the support structure design on the cell performance, the relative magnitude of all the various losses in each type of SOFC is given in Fig. 3b. The data show that the ohmic loss dominates the performance of the electrolyte-supported SOFC whereas activation and ohmic overpotentials are the major loss in the electrode-supported counterpart. By comparing the various cell voltage losses, it is observed that the concentration loss is relatively small, even though the SOFC is supported by the electrode. Nevertheless, the concentration loss becomes more significant for the cathode-supported cell as a rapid drop of the cell voltage is observed at a current density of 2.8 A cm^{-2}. Under this operating condition, a large amount of oxidant is consumed at the cathode|electrolyte interface and, therefore, the concentration loss is increasingly developed. From simulation results, it can be concluded that the anode-supported SOFC exhibits better performance in comparison with the others; it can be operated at high current density and a greater power density is achieved. Further, Fig. 3a shows that there is a possibility to improve the performance of the anode-supported SOFC as the limiting current density at the anode is still not reached. Therefore, in the next section, the effect of structural and operating parameters on the performance of an anode-supported SOFC are further investigated.

3.2. *Effect of electrolyte thickness*

In this section, the impact of the electrolyte thickness on the performance of an anode-supported SOFC is analyzed. The electrolyte thickness varies from 10 to 40 μm while the anode and cathode thicknesses are fixed at 500 and 40 μm, as in the

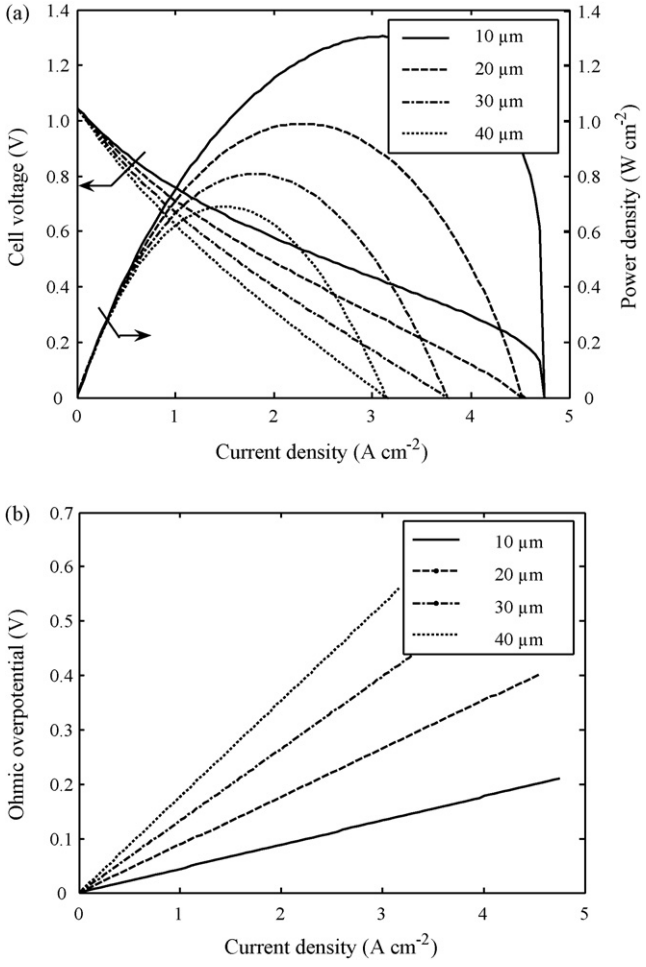

Fig. 4. Effect of electrolyte thickness at different current densities on (a) cell voltage and power density and (b) ohmic overpotential.

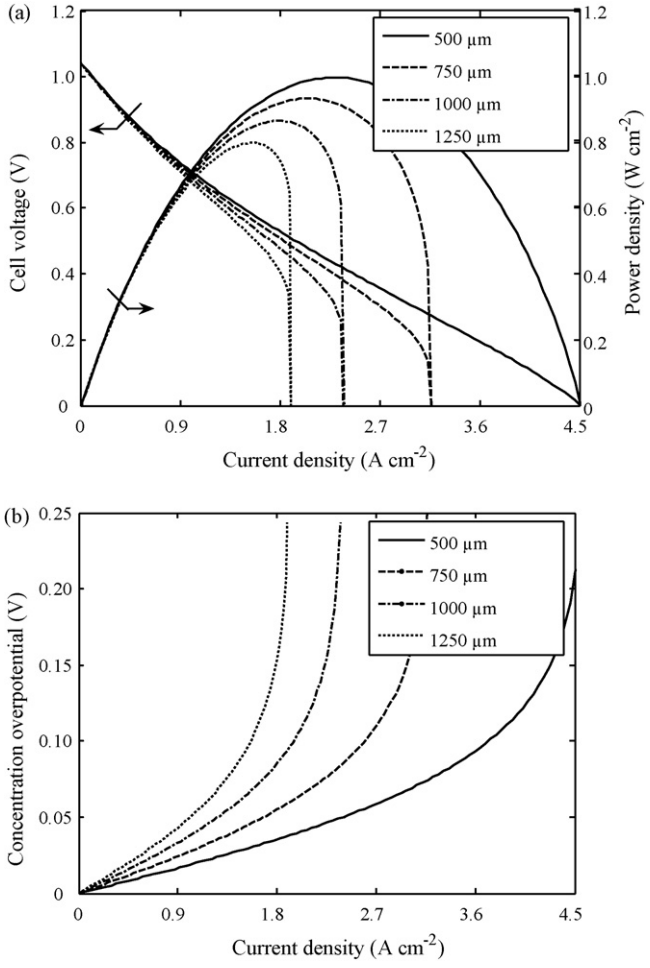

Fig. 5. Effect of anode thickness at different current densities on (a) cell voltage and power density and (b) concentration overpotential.

standard specification, respectively. The cell voltage and power density as a function of current density at different electrolyte thicknesses are given in Fig. 4a. For each value of electrolyte thickness, there is an optimum current density and hence a maximum power density; the current density corresponding to the maximum power density is moved to higher values with decrease in the electrolyte thickness. Thus, as expected, the cell performance increases when the electrolyte thickness decreases. This is because the decrease of the electrolyte thickness causes a significant decrease in the ohmic overpotential as shown in Fig. 4b. By contrast, the anode concentration overpotential becomes a more significant loss when a thinner electrolyte is used. As can be seen in Fig. 4a, the voltage of the anode-supported SOFC with an electrolyte thickness of 10 μm rapidly decreases at a current density of 4.7 A cm^{-2} due to a high anode concentration overpotential; a concave curvature is observed.

3.3. Effect of anode thickness

Fig. 5a presents the characterization curve of an anode-supported SOFC at different anode thicknesses (500, 750, 1000 and 1250 μm). It is noted that the electrolyte and cathode thicknesses are fixed at 20 and 40 μm, respectively. The results show that the cell performance is significantly hindered when the anode thickness increases (Fig. 5a). The latter causes a higher resistance to the gaseous species being transported in the porous anode, and this results in an exponential increase in the concentration overpotential (Fig. 5b). It can be further observed that the concentration overpotential in an anode-supported SOFC with a larger anode thickness has a significant effect on cell performance; the maximum operating current density appears to approach the limiting current density of the anode.

3.4. Effect of cathode thickness

The effect of cathode thickness (25, 40, 100 and 150 μm) on the performance of an anode-supported planar SOFC at different current densities has been investigated. The simulation results demonstrate that the thickness of the cathode has less influence on the characteristic curve of the fuel cell; the concentration and ohmic overpotentials decrease slightly with reduction in cathode thickness.

3.5. Effect of operating temperature

The characteristic curve of cell voltage and power density for an anode-supported SOFC at different operating temperatures is presented in Fig. 6a. The individual overpotentials are shown in Fig. 6b–d. As expected, the cell performance decreases drastically with decreasing operating temperature. This is mainly caused by an increase in both the ohmic overpotential (Fig. 6b) and the activation overpotential (Fig. 6c). The effect of operating temperature on the concentration overpotential is shown in Fig. 6d. The concentration overpotential exhibits a large increase when the fuel cell is operated at 1273 K and this causes the cell voltage to drop to zero at a the current density of 4.0 A cm^{-2}. It should be noted that although the anode-supported SOFC, which has thinner electrolyte and is suitable for low temperature opera-

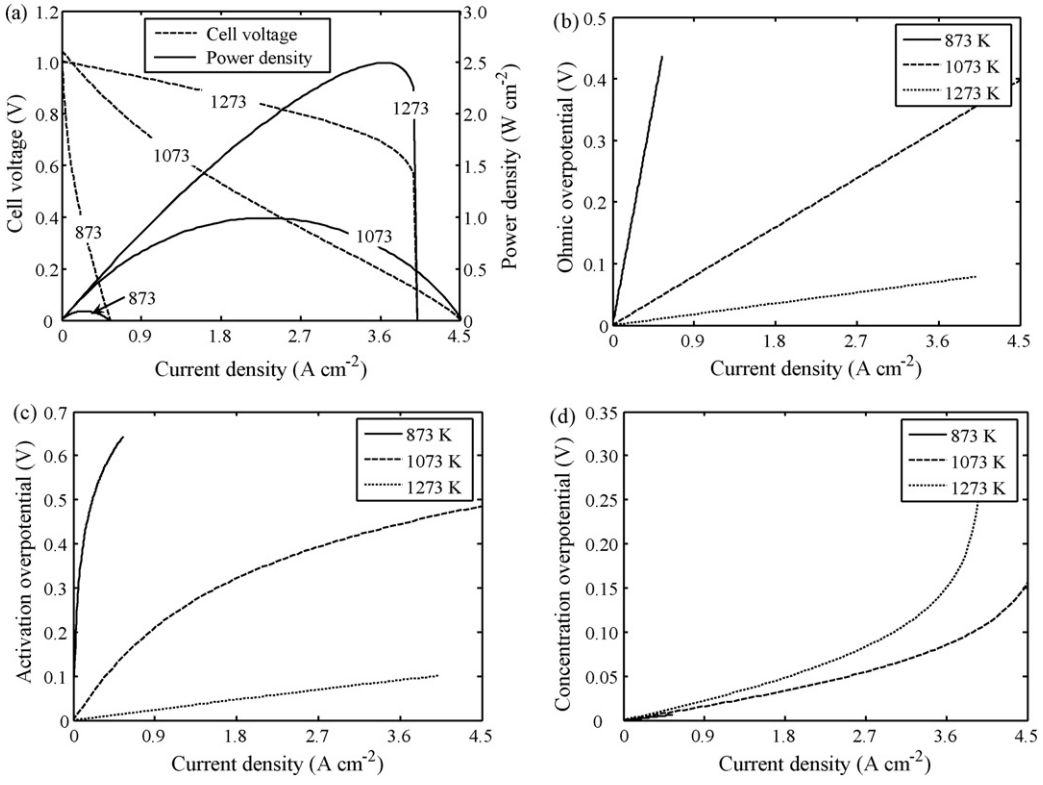

Fig. 6. Effect of operating temperature at different current densities on (a) cell voltage and power density, (b) ohmic overpotential, (c) activation overpotential and (d) concentration overpotential.

tion, is used with the aim to decrease an ohmic overpotential, the loss is still relatively major in the fuel cell. In order to improve SOFC performance, an electrolyte with high ionic conductivity is required.

3.6. Effect of operating pressure

The effect of operating pressure on the characteristic curve of a SOFC is shown in Fig. 7a, in which the operating pressure is varied from 0.5 to 3 atm. Cell performance increases with increase in operating pressure. At high pressure operation, fuel and oxidant gases can easily diffuse to the electrode|electrolyte interface and therefore, the concentration overpotential is reduced as can be seen in Fig. 7b

3.7. Effect of fuel composition

Fuel composition is a further key parameter that needs to be considered. The impact of fuel composition on cell performance is studied by varying the degree of pre-reforming of methane at 10, 30, 50 and 70%. It is noted that a higher degree of pre-reforming results in an increase in the H_2 concentration in the fuel composition. Fig. 8a illustrates that increasing the degree

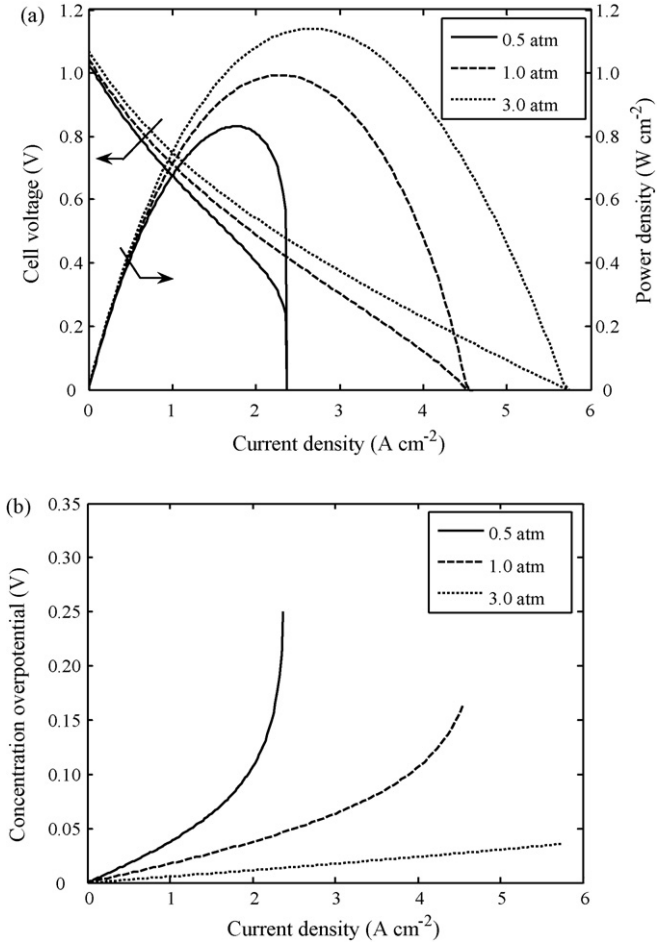

Fig. 7. Effect of operating pressure at different current densities on (a) cell voltage and power density and (b) concentration overpotential.

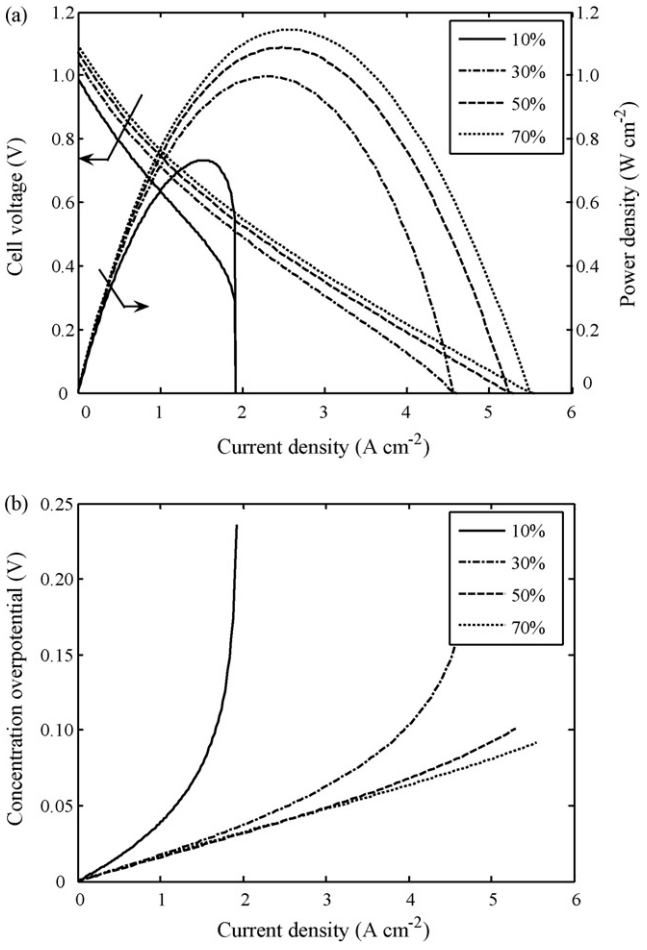

Fig. 8. Effect of % pre-reforming at different current densities on (a) cell voltage and power density and (b) concentration overpotential.

of pre-reforming of fuel can improve the cell performance, i.e., a higher operating current density can be achieved. High-hydrogen fuel increases the open-circuit voltage (Eq. (1)) and significantly decreases the concentration overpotential (Fig. 8b) as more H_2 is able to move to the electrode|electrolyte interface. On the other hand, a change in fuel composition does not affect either the ohmic or the activation overpotential.

4. Conclusions

A numerical study of the performance of a SOFC with different support structures has been presented. A detailed electrochemical model in which the effects of structural and operational parameters and also gas diffusion at the electrodes are taken into consideration is employed to determine the characteristic performance of the SOFC. Under intermediate-temperature operation, it is found that an electrode-supported SOFC exhibits better electrical performance than an electrolyte-supported SOFC. Considering individual cell voltage loss, the results indicate that ohmic loss dominants the performance of the electrolyte-supported SOFC, whereas activation and ohmic overpotentials constitute the major loss in an electrode-supported SOFC. Compared with the cathode-supported SOFC, the anode-supported SOFC delivers better performance in terms

of a wider range of operating current density; the concentration loss becomes more significant for a cathode-supported cell as a rapid drop of the cell voltage is observed at high current density.

Sensitivity analyses of the anode-supported SOFC have been performed. The results demonstrate that decreasing the electrolyte and anode thickness can improve cell performance, whereas the cathode thickness has less effect on the cell characteristic curve. It is also found that a decrease in operating temperature causes the cell to operate at a lower range of current density due to an increase in both the ohmic and the activation overpotentials. Further, an increase in operating pressure and the degree of pre-reforming reduces concentration overpotential, which result in enhanced cell performance.

References

[1] X. Xue, J. Tang, N. Sammes, Y. Du, J. Power Sources 142 (2005) 211–222.
[2] S.C. Singhal, Solid State Ionics 152/153 (2002) 405–410.
[3] J.H. Hirschenhofer, D.B. Stauffer, R.P. Engleman, M.G. Klett, Fuel Cell Handbook, 4th edition, U.S. Department of Energy, 1998.
[4] P. Costamagna, A. Selimovic, M.D. Borghi, G. Agnew, Chem. Eng. J. 102 (2004) 61–69.
[5] N.Q. Minh, T. Takahashi, Science and Technology of Ceramic Fuel Cells, Elsevier, New York, USA, 1995.
[6] H. Yakabe, T. Ogiwarw, M. Hishinuma, I. Yasuda, J. Power Sources 102 (2001) 144–154.
[7] A.V. Virkar, J. Chen, C.W. Tanner, J. Kim, Solid State Ionics 131 (2000) 189–198.
[8] S. Kakaç, A. Pramuanjaroenkij, X.Y. Zhou, Int. J. Hydrogen Energ. 32 (2007) 761–786.
[9] E. Achenbach, J. Power Sources 49 (1994) 333–348.
[10] P. Aguiar, D. Chadwick, L. Kershenbaum, Chem. Eng. Sci. 57 (2002) 1665–1677.
[11] M. Ni, M.K.H. Leung, D.Y.C. Leung, Energ. Convers. Manage. 48 (2007) 1525–1535.
[12] P. Aguiar, C.S. Adjiman, N.P. Brandon, J. Power Sources 138 (2004) 120–136.
[13] J.R. Ferguson, J.M. Fiard, R. Herbin, J. Power Sources 58 (1996) 109–122.
[14] T. Setoguchi, K. Okamoto, K. Eguchi, H. Arai, J. Electrochem. Soc. 139 (1992) 2875–2880.
[15] S.P. Jiang, S.P.S. Badwal, J. Electrochem. Soc. 144 (1997) 3777–3784.
[16] K.R. Thampi, A.J. McEvoy, J. Van herle, J. Electrochem. Soc. 142 (1995) 506–513.
[17] J.W. Kim, A.V. Virkar, K.Z. Fung, K. Mchta, S.C. Singhal, J. Electrochem. Soc. 146 (1999) 69–78.